ELSEVIER

Journal of Hazardous Materials 130 (2006) 88–106

Journal of Hazardous Materials

www.elsevier.com/locate/jhazmat

Kinetics of acid-catalyzed cleavage of cumene hydroperoxide

M.E. Levin [a,*], N.O. Gonzales [a], L.W. Zimmerman [a], J. Yang [b]

[a] *Shell Global Solutions (US) Inc., P.O. Box 1380, Houston, TX 77251 1380, USA*
[b] *Shell Chemical LP, P.O. Box 4327, Houston, TX 77210, USA*

Available online 25 October 2005

Abstract

The cleavage of cumene hydroperoxide, in the presence of sulfuric acid, to form phenol and acetone has been examined by adiabatic calorimetry. As expected, acid can catalyze cumene hydroperoxide reaction at temperatures below that of thermally-induced decomposition. At elevated acid concentrations, reactivity is also observed at or below room temperature. The exhibited reactivity behavior is complex and is significantly affected by the presence of other species (including the products). Several reaction models have been explored to explain the behavior and these are discussed.

Keywords: Acid-catalyzed cleavage; Cumene hydroperoxide; Adiabatic calorimetry

1. Introduction

1.1. Background

An important process for producing oxygenated hydrocarbons from petrochemical feedstocks is the formation and oxidation of relatively easily peroxidized species coupled with their ensuing decomposition. One such process entails the oxidation of cumene to cumene hydroperoxide (CHP) followed by the acid-catalyzed cleavage to form phenol and acetone. The cumene itself is generated by acid-catalyzed alkylation of benzene with propylene.

It is well recognized that organic hydroperoxides are subject to decomposition upon exposure to heat, acids, bases, metals, contaminants, etc. [1–5]. When unanticipated and/or uncontrolled, serious safety incidents can occur threatening loss of life, damage to facilities, and interruption to business. Numerous such incidents have been experienced in industry with cumene hydroperoxide [6,7]. For this reason, it is vital that the behavior of hydroperoxides being handled is understood and that the risks associated with their reactivity are managed.

The reaction pathways of cumene hydroperoxide are plentiful and complex. Many reactions arise from free radical mechanisms leading to a wide variety of products. A few of the essential reaction paths and products are illustrated in Fig. 1. Two primary reactions occur simply from exposure of the hydroperoxide to elevated temperature to form (1) dimethyl benzyl alcohol (DMBA) through reaction with cumene and (2) acetophenone plus methanol. The acid-catalyzed route to phenol and acetone mentioned above is also depicted. Many past literature studies have examined and employed various aspects of the energetics and kinetics of CHP reactions [8–12]. This study examines these particular pathways and their associated kinetics.

1.2. Approach

In this study, the reactive behavior of cumene hydroperoxide alone and with injected amounts of sulfuric acid has been examined through use of adiabatic calorimetry. Through measurement of heat release and pressure generation, this approach provides the opportunity to observe and characterize in a laboratory setting the accelerating reaction environment that might be experienced in an industrial-scale event.

2. Experimental

2.1. Equipment

Testing for this study was carried out in the Automatic Pressure Tracking Adiabatic Calorimeter (APTAC^{TM}) available from TIAX, LLC, described in previous studies [13,14]. The instrument operates on the principle of minimizing the heat loss from the sample and $2\frac{1}{2}$ in. diameter sample cell by heating

* Corresponding author. Tel.: +1 281 544 7575; fax: +1 281 544 7705.
E-mail address: marc.levin@shell.com (M.E. Levin).

0304-3894/$ – see front matter © 2005 Published by Elsevier B.V.
doi:10.1016/j.jhazmat.2005.07.068

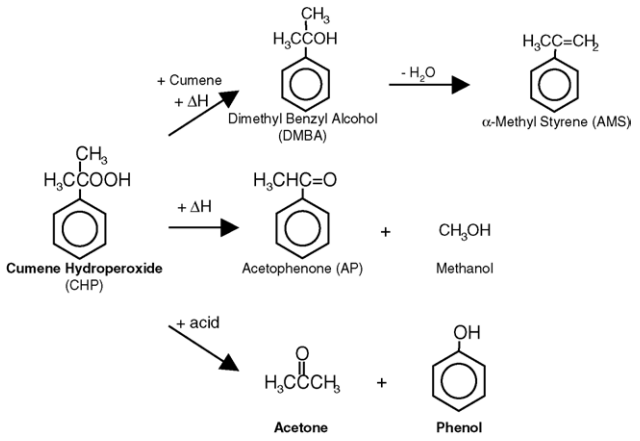

Fig. 1. Selected reaction pathways of cumene hydroperoxide.

the gas space surrounding the cell to match the sample temperature, as measured by an internal thermocouple. This allows a sample undergoing an exothermic reaction to self-heat at a rate and extent comparable to that in a large-scale adiabatic environment. The APTAC heaters and containment vessel pressurization control can match temperature and pressure rise rates of up to 400 °C/min and 10,000 psi/min, respectively. To reduce the possibility of metal-catalyzed reaction, glass equipment is employed where possible. Stirring in this study is accomplished via a glass-encapsulated magnetic stir bar inserted in a sodium borosilicate sample cell. The sample thermocouple is also isolated from the cumene hydroperoxide by means of a glass capillary sealed on one end.

The relative thermal capacitance of the cell plus sample to the sample alone is expressed by the thermal inertia factor, ϕ,

$$\phi = 1 + \frac{m_c C_{p_c}}{m_s C_{p_s}}$$

where m denotes the mass, C_p the heat capacity, subscript c the cell + stir bar, and s the sample. The ϕ factor of commercial equipment approaches a value of 1; a value of 1.25–1.35 is typical of APTAC tests utilizing 30–45 g sodium borosilicate glass cells.

Operation is typically in the heat-wait-search mode. That is, the sample is heated to a pre-selected temperature and upon reaching this temperature, the instrument waits for a period of time (usually 25 min) for the cell and containment vessel temperatures to stabilize. After the wait period, the instrument "searches" at that temperature (for another 25 min) for any exothermic activity. During this time, the temperature of the containment vessel gas space is adjusted to match that of the sample thermocouple. If no heat-up activity exceeding a pre-set self-heating rate threshold is observed, it is concluded that there is no exotherm. The sample is then heated to the next temperature and the process repeated. If an exotherm is detected, the APTAC tracks the sample conditions and adjusts the temperature and pressure of the containment vessel accordingly (adiabatic or exotherm mode).

APTAC exotherm thresholds of 0.05–0.06 °C/min are employed to reduce the likelihood of the occurrence of "drift" (in which a slight thermocouple calibration imbalance yields a slow, artificial temperature rise rate and is interpreted as an exotherm).

2.2. Samples

2.2.1. Cumene hydroperoxide

Cumene hydroperoxide samples of various concentrations were obtained from sampling points on existing manufacturing units. Samples of about 11.3, 20.6, and 83.9 wt% CHP were obtained from a unit that operates in a slightly alkaline environment ("Source #1"). Samples of 11.7, 24.6, and 82.5 wt% CHP were drawn from another unit whose conditions are somewhat acidic ("Source #2"). The balance of species in the samples is primarily cumene with minor amounts of dimethyl benzyl alcohol, acetophenone, and alpha methyl styrene (Table 1).

2.2.2. Acid catalyst

Sulfuric acid of 95–98 wt% strength was obtained from Sigma–Aldrich (catalog number 33,974-1). In dosing the sample with sulfuric acid, water was avoided since it is known to significantly impact the activity of the acid. For the low concentration (200 ppmw) sulfuric acid case, the sulfuric acid was simply added to *n*-tridecane (catalog number T5,740-1 from Sigma–Aldrich), assuming that the acid would solubilize in the tridecane. For higher concentration tests (e.g., 2000 ppmw and higher), neat sulfuric acid was injected, followed by *n*-tridecane employed as a "chase" material to facilitate the transfer of all acid into the sample cell.

Table 1
Composition of cumene hydroperoxide samples

Sample	Manufacturing environment					
	Source #1 Slightly alkaline			Source #2 Slightly acidic		
	1 (wt%)	2 (wt%)	3 (wt%)	1 (wt%)	2 (wt%)	3 (wt%)
Cumene hydroperoxide (CHP)	11.3	20.6	83.9	11.7	24.6	82.5
Cumene	86.6	75.5	5.6	85.8	72.0	10.8
Dimethylbenzyl alcohol (DMBA)	1.2	1.8	8.0	0.5	1.4	1.3
Acetophenone (AP)	0.12	0.19	0.65	0.12	0.12	0.37
Alpha methyl styrene (AMS)	0.02	0.02	0.02	0.02	0.02	0.02

2.2.3. Other materials

Also employed in this study were neat acetone (Sigma–Aldrich, #32011-0, 99.5%), cumene (Sigma–Aldrich, #18,579-5, 99.5%), phenol (Sigma–Aldrich, P-5566, >99.5%), and ethylbenzene sulfonic acid (Sigma–Aldrich, #24,520-8, 95%).

2.3. Procedures

2.3.1. Cumene hydroperoxide sample addition

For each test, a clean sodium borosilicate glass cell was fitted with a septum, purged with nitrogen, and placed in a nitrogen-purged glove box containing the appropriate cumene hydroperoxide and other hydrocarbon samples. Inside the glove box, the septum was removed, the selected amounts of cumene hydroperoxide and hydrocarbons were then added to the cell, and the septum then re-inserted on the cell.

2.3.2. APTAC mounting

To limit exposure to air (and possible oxidation side reactions), the septum-sealed glass sample cell was placed inside a glove bag. The glove bag was then secured to the containment vessel head and the interior purged five times successively with nitrogen (each time followed by evacuation via house vacuum). The septum was then removed from the glass sample cell, the cell was mounted onto the containment vessel head, and the cell nut was then tightened. Once the cell was firmly attached, the glove bag was removed, the nut tightness checked, and the containment vessel closed.

2.3.3. Sulfuric acid injection

Due to the anticipated rapid reaction of cumene hydroperoxide at ambient temperature in the presence of sulfuric acid, the acid was manually injected just after test initiation. Two parallel, glass syringes were set up for this purpose. One syringe contained sulfuric acid with *n*-tridecane; the other contained only *n*-tridecane. The syringes were oriented vertically so that the barrel was above the needle. In this arrangement, the lower density tridecane would naturally rest above the sulfuric acid in the acid syringe and would be injected last. The two syringes were connected through a tee to 1/16 in. tubing going to the sample cell via the APTAC tube heater assembly. All tubing employed was type 316 stainless steel and the associated fittings were type 316 stainless steel. The sulfuric acid plus tridecane in the first syringe was quickly and smoothly injected. This

Table 2
Thermal decomposition tests (Source #1)

	Run ID				
	A00536	A00534	A00535	A00537	A00538
LR	LR25305-35	LR25305-33	LR25305-34	LR25305-37	LR25305-40
CHP concentration (wt%)	11.3	20.6	20.6	83.9	83.9
CHP + cumene sample mass (g)	60.01	60.12	60.00	60.12	60.07
Sample cell mass (glass) (g)	33.03	32.29	31.40	31.39	32.16
Stir bar mass (g)	2.01	2.04	2.04	2.02	1.88
Stirring rate (magnetic) (rpm)			500		
Experiment (search) start temperature (°C)			50		
Experiment final or maximum temperature (°C)			300		
Heat-wait-search increment (°C)			10		
Experiment exotherm limit (N_2) (°C)			300		
Experiment temperature shutdown (°C)			325		
Experiment pressure shutdown (psia)			1800		
Experiment heat rate shutdown (°C/min)			800		
Experiment pressure rate shutdown (psi/min)			1000		
Exotherm threshold (°C/min)			0.06		
Number of exotherms[a]	1	1	1+	1+	1+
Initial observed exotherm temperature (°C)	131	122	122	111	112
Maximum observed temperature (°C)	178	203	236	413	428
Maximum observed pressure (psia)	200	239	741	534	671
Maximum observed self-heat rate (°C/min)	0.58	16.9	16.9	6290	7570
Maximum observed pressure rate (psi/min)	1.9	60.0	79.9	14,800	18,800
Temperature at maximum self-heat rate (°C)	163	203	203	386	397
Temperature at maximum pressure rate (°C)	168	203	224	337	226
Raw adiabatic temperature rise (°C)	47.3	88	114	302+	316+
Thermal inertia, ϕ	1.26	1.26	1.25	1.29	1.29
Experiment duration (before shutdown) (min)	1706	673	1048	642	583
Experiment shutdown (S/D) cause	Exo limit *T*	Unknown	Exo limit *T*	*T*, *P* rate	*T*, *P* rate
Composition measured in product liquid	Yes		Yes		
Comments		Test ended prematurely, possibly due to cell breakage		Cell ruptured during test	Cell ruptured during test

[a] In some tests, the shape of the self-heat rate curve vs. reciprocal temperature suggests the possibility of an additional exotherm.

Table 3
Thermal decomposition tests (Source #2)

	Run ID					
	A00540	A00597	A00547	A00596	A00599	A00548
LR	LR25305-45	LR25703-76	LR25305-59	LR25703-75	LR25703-79	LR25305-61
CHP concentration (wt%)	11.7	11.7	24.6	23	23.9	82.5
CHP + cumene sample mass (g)	60.06	59.94	60.49	60.00	60.00	60.03
Sample cell mass (glass) (g)	33.96	34.00	33.99	36.79	36.80	30.20
Stir bar mass (g)	1.88	1.95	1.90	1.95	1.93	1.89
Stirring rate (magnetic) (rpm)				500		
Experiment (search) start temperature (°C)				50		
Experiment final or maximum temperature (°C)				300		
Heat-wait-search increment (°C)				10		
Experiment exotherm limit (N_2) (°C)				300		
Experiment temperature shutdown (°C)				325		
Experiment pressure shutdown (psia)				1800		
Experiment heat rate shutdown (°C/min)				800		
Experiment pressure rate shutdown (psi/min)				1000		
Exotherm threshold (°C/min)				0.06		
Number of exotherms[a]	1+	1+	1+	1	1	1+
Initial observed exotherm temperature (°C)	111	131	122	122	133	101
Maximum observed temperature (°C)	209	194	269	245	258	408
Maximum observed pressure (psia)	257	209	592	408	523	844
Maximum observed self-heat rate (°C/min)	2.4	0.95	74	26.4	35.6	5910
Maximum observed pressure rate (psi/min)	9.3	3.0	393	134	180	2200
Temperature at maximum self-heat rate (°C)	187	173	248	229	236	380
Temperature at maximum pressure rate (°C)	190	180	253	229	241	244
Raw adiabatic temperature rise (°C)	97	62	147	124	125	307+
Thermal inertia, ϕ	1.26	1.27	1.27	1.29	1.29	1.28
Experiment duration (before shutdown) (min)	1284	1258	791	723	903	612
Experiment shutdown (S/D) cause	Manual S/D	Manual S/D	Exo limit *T*	Uncertain	Exo limit *T*	*T*, *P* rate
Composition measured in product liquid	Yes		Yes		Yes	
Comments	Instrument drift			Possibly premature end		Cell ruptured

[a] In some tests, the shape of the self-heat rate curve vs. reciprocal temperature suggests the possibility of an additional exotherm.

was then followed by injection of the tridecane in the second syringe. The syringes were then quickly isolated from the cell by use of block valves in the 1/16 in. tubing.

Total sample weights ranged from 59.9 to 63.7 g, while the total weight of glass cell and stir bar ranged between 32.1 and 40.3 g. A summary of test characteristics may be found in Tables 2–5.

2.3.4. Compositional analyses

Feed mixtures and selected test liquid product were analyzed by gas chromatography (GC) equipped with a flame ionization detector. Co-elution with the GC solvent masked measurement of the acetone concentration. In two cases (tests A00614 and A00616), liquid product was analyzed by NMR. No gas samples for compositional analysis were taken at the end of any of the tests.

3. Results and discussion

3.1. Thermal decomposition of CHP

The reactivity of cumene hydroperoxide is illustrated in Fig. 2a and b in terms of temperature rise. Fig. 2a depicts the temperature versus time results for several CHP concentrations ranging from 11.3 to 83.9 wt% in a slightly alkaline environment. Fig. 2b shows the corresponding behavior for 11.7–82.5 wt% CHP in a slightly acidic environment. As expected, in both cases, the extent of temperature rise is greater for the higher concentration CHP samples. The stair-step behavior seen in the experiment temperature–time traces arises from the heat-wait-search mode before (and after) the main exotherm. From these figures, it is evident that reaction is detected when the temperature is around 100 °C or higher. Temperatures greater than 420 °C can be achieved for the high concentration samples. Some subtle differences exist between the behavior of material in the alkaline environment and that in the acidic environment.

The corresponding pressure versus time histories are depicted in Fig. 3a and b. The amount of pressure developed during the course of reaction depends directly on the amount of CHP present. Pressures approaching 700 psia can be generated upon decomposition of high concentrations of CHP.

The rate of CHP decomposition is reflected in the self-heat rate versus reciprocal temperature plots of Fig. 4a and b. For clarity, these data are plotted without the heat-wait-search steps. For Arrhenius-type kinetics, the initial slopes in the self-heat rate versus reciprocal temperature plot relate to the activation energy of the reaction. The rate ultimately reaches a maximum as reactant is depleted and quickly diminishes. It is clear from these

Table 4
Sulfuric acid-catalyzed tests

	Run ID						
	A00600	A00601	A00606	A00607	A00603	A00602	A00616
LR	LR25703-79	LR25703-80	LR25703-85	LR25703-86	LR25703-82	LR25703-81	LR25703-100
CHP concentration (Source #2) (wt%)	24.6	24.6	24.6	24.6	24.6	24.6	4.3
CHP + cumene sample mass (g)	56.41	58.26	58.33	58.29	58.00	56.75	57.95
Sulfuric acid concentration (wt%)	0.020	0.184	0.510	0.518	0.816	1.932	0.798
Sulfuric acid mass (g)	0.0123	0.1124	0.3125	0.317	0.500	1.183	0.488
Tridecane mass (g)	3.599	1.624	1.402	1.394	1.557	2.056	1.539
Sample cell mass (glass) (g)	36.80	36.80	36.80	36.80	36.80	36.86	34.61
Stir bar mass (g)	1.98	2.00	1.90	1.91	1.82	1.91	1.83
Stirring rate (magnetic) (rpm)	500	500	500	500	500	500	500
Experiment (search) start temperature (°C)	20	20	20	20	20	20	20
Experiment final or maximum temperature (°C)	300	300	240	240	240	300	40
Heat-wait-search increment (°C)	10	10	5	5	5	5	5
Experiment exotherm limit (N_2) (°C)	300	300	250	250	250	300	250
Experiment temperature shutdown (°C)	325	325	325	325	325	325	45
Experiment pressure shutdown (psia)	1800	1800	1800	1800	1800	1800	1800
Experiment heat rate shutdown (°C/min)	800	800	800	800	800	800	800
Experiment pressure rate shutdown (psi/min)	1000	1000	1000	1000	1000	1000	1000
Exotherm threshold (°C/min)	0.05	0.05	0.05	0.05	0.05	0.05	0.05
Number of exotherms[a]	1+	1+	3	3	3	3	2+
Initial observed exotherm temperature (°C)	102	83	21	9	8	7	10
Maximum observed temperature (°C)	222	214	174	173	160	172	36
Maximum observed pressure (psia)	387	211	110	110	67	60	13
Maximum observed self-heat rate (°C/min)	50.5	223	201	199	435	2570	42
Maximum observed pressure rate (psi/min)	207	561	83	58	43	41	0.12
Temperature at maximum self-heat rate (°C)	200	195	21	18	27	154	13
Temperature at maximum pressure rate (°C)	205	202	162	160	70	166	36
Raw adiabatic temperature rise (°C)	119	131	154	164	151	166	27
Thermal inertia, ϕ	1.30	1.30	1.31	1.31	1.31	1.31	1.27
Experiment duration (before shutdown) (min)	989	951	169	746	31	0.6	14
Experiment shutdown (S/D) cause	Manual S/D	Manual S/D	Manual S/D	Exo search T	Heaters	Uncertain	Manual S/D
Composition measured in product liquid	Yes	Yes		Yes	Yes	Yes	Yes
Comments	Drift		Data collection begun at 21 °C		Heaters not engaged	Cell ruptured	

[a] In some tests, the shape of the self-heat rate curve vs. reciprocal temperature suggests the possibility of an additional exotherm.

plots that higher reactivity accompanies the higher concentration CHP samples. This appears as a lower temperature for detection of reaction as well as a substantially higher peak self-heat rate. In addition to the rate dependence on the CHP concentration itself, the higher peak rate is a direct result of the higher temperature achieved by reaction of higher concentration combined with the effect of Arrhenius-type kinetics. It should be noted that the increased rate associated with test A00597, as compared with A00540, arises from the presence of some positive instrument drift superimposing on the reaction rate. Also, the shape of the self-heat rate curves in some tests show subtle signs of multiple peaks, such as the shoulders appearing for tests A00535 and A00547.

Peak self-heat rates of the order of 6000–8000 °C/min are observed for the >80 wt% CHP samples. In actuality, higher rates could possibly have taken place had the sample cells not usually ruptured during the high CHP concentration experiments. For self-heat rates above 1000 °C/min, there is a flattening of the self-heat rate versus reciprocal temperature slope possibly a result of time lag in the sample thermocouple. Moreover, heat loss from the sample cell increases as the heaters fail to match the sample temperature at high self-heat rates. Because of these factors, observed self-heat rates much greater than 100 °C/min can be assumed to have been even higher under more adiabatic and better controlled conditions.

Table 5
Additional sulfuric acid-catalyzed tests

	Run ID						
	A00605	A00614	A00630	A00635	A00629	A00632	A00634
LR	LR25703-84	LR25703-96	LR25703-119	LR25703-126	LR25703-118	LR25703-120	LR25703-125
CHP concentration (Source #2) (wt%)	10	10	10	10	10	10	10
CHP + cumene sample mass (g)	57.97	57.97	27.82	37.69	7.55	57.00 + 7.55	57.50
Phenol mass (g)	0	0	30.16	0	30.18	[a]	0
Acetone mass (g)	0	0	0	20.29	20.32	[a]	0
Sulfuric acid concentration (wt%)	0.829	0.805	0.802	0.800	0.800	0.702	0.782[a]
Sulfuric acid mass (g)	0.508	0.493	0.491	0.490	0.490	0.464	0.968[a]
Tridecane mass (g)	1.534	1.535	1.542	1.535	1.542	1.135	1.538
Sample cell mass (glass) (g)	36.86	35.11	38.36	37.34	38.36	37.77	37.77
Stir bar mass (g)	1.82	1.84	1.96	1.92	1.96	1.97	1.92
Stirring rate (magnetic) (rpm)	500	500	500	500	500	500	500
Experiment (search) start temperature (°C)	20	20	20	20	20	20	20
Experiment final or maximum temperature (°C)	240	85	160	240	240	240	240
Heat-wait-search increment (°C)	5	5	5	5	5	10	10
Experiment exotherm limit (N_2) (°C)	250	250	250	250	250	250	250
Experiment temperature shutdown (°C)	325	325	325	325	325	325	325
Experiment pressure shutdown (psia)	1800	1800	1800	1800	1800	1800	1800
Experiment heat rate shutdown (°C/min)	800	800	2500	2500	800	2500	2500
Experiment pressure rate shutdown (psi/min)	1000	1000	1000	1000	1000	1000	1000
Exotherm threshold (°C/min)	0.05	0.05	0.05	0.05	0.05	0.05	0.05
Number of exotherms[b]	3	2+	2+	3	2+	2+	2+
Initial observed exotherm temperature (°C)	8	7	12	8	5	3	8
Maximum observed temperature (°C)	69	75	83	78	74	62	76
Maximum observed pressure (psia)	20	17	16	34	27	27	22
Maximum observed self-heat rate (°C/min)	111	132	1640	74	1180	58	348
Maximum observed pressure rate (psi/min)	0.15	0.30	0.3	1.3	2.2	0.40	1.5
Temperature at maximum self-heat rate (°C)	15	13	70	13	64	11	23
Temperature at maximum pressure rate (°C)	36	75	81	77	71	61	72
Raw adiabatic temperature rise (°C)	60	67	72	69	68	58	67
Thermal inertia, ϕ	1.29	1.27	1.31	1.30	1.30	1.28	1.30
Experiment duration (before shutdown) (min)	1122	101	105	1921	0.50	110	1.3
Experiment shutdown (S/D) cause	Manual S/D	Manual S/D	Manual S/D	Maximum Search *T*	Manual S/D	Manual S/D	Manual S/D
Composition measured in product liquid		Yes					
Comments		Restart of test after heaters shut off				7.55 g of 82.5 wt% CHP sample injected into liquid product of A00631	

[a] From product of test A00631.
[b] In some tests, the shape of the self-heat rate curve vs. reciprocal temperature suggests the possibility of an additional exotherm.

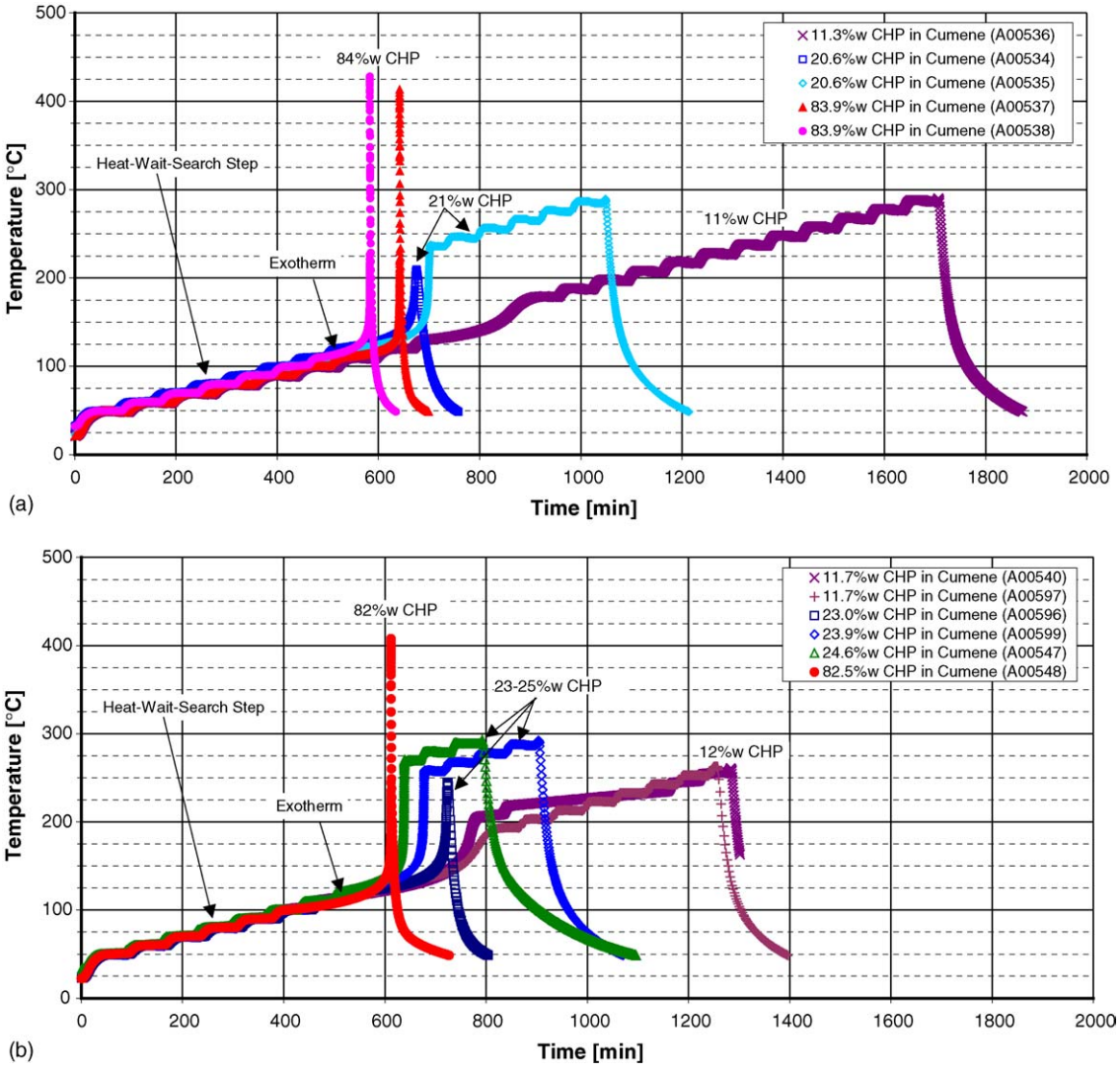

Fig. 2. Temperature–time history for CHP thermal decomposition. APTAC experiments; in nitrogen: (a) Source #1 and (b) Source #2.

The pressurization rate versus reciprocal temperature profiles for CHP thermal decomposition are displayed in Fig. 5a and b. The same general trend of higher rate for increased CHP concentration is observed. A closer look also reveals that the slope of pressurization rate changes, becoming steeper around 160 °C. This behavior suggests a possible shift in reaction path.

The pressure–temperature profiles of Fig. 6a and b demonstrate the generation of non-condensible species during reaction. The residual pressure upon cool-down to 50 °C (at which point instrument data collection halted) is substantially higher than at the same temperature during heat-up. Note that test A00534 ended prematurely, possibly due to damage to the cell neck (chipping) resulting in slight depressurization of the cell to the containment vessel pressure, and thereby heat loss to quench the reaction (which had nearly peaked).

As an indication of the available response time for handling CHP thermal decomposition, Fig. 7a and b depict the time to maximum rate for the various CHP concentrations in relation to the material temperature. For example, for the 83.9 wt% CHP sample from Source #1 at a temperature of 120 °C, it would take only 35 min to reach the peak heat rate. All of the samples show comparable behavior, with somewhat parallel slopes. As expected, the available time for high concentrations of CHP is considerably less than that for low concentrations at the same temperature.

Liquid product concentrations from selected tests are presented in Table 6. In the lower half of the table, the concentrations are given on a normalized, cumene-free basis. It is clear that, in all cases, the vast majority of CHP has been converted during the tests and that little CHP was cleaved to phenol plus acetone. Taking into account the stoichiometry of the thermal decomposition reactions (as well as the dehydration to α-methyl styrene), it can be shown that about 40–50% of the CHP (on a molar basis) reacted to form dimethylbenzyl alcohol. Roughly 50–60% of the CHP formed acetophenone.

To generate kinetics that describe the thermal decomposition of CHP, SAFIRE (the two-phase dynamic relief evaluation software formerly sold by the American Institute of Chemical

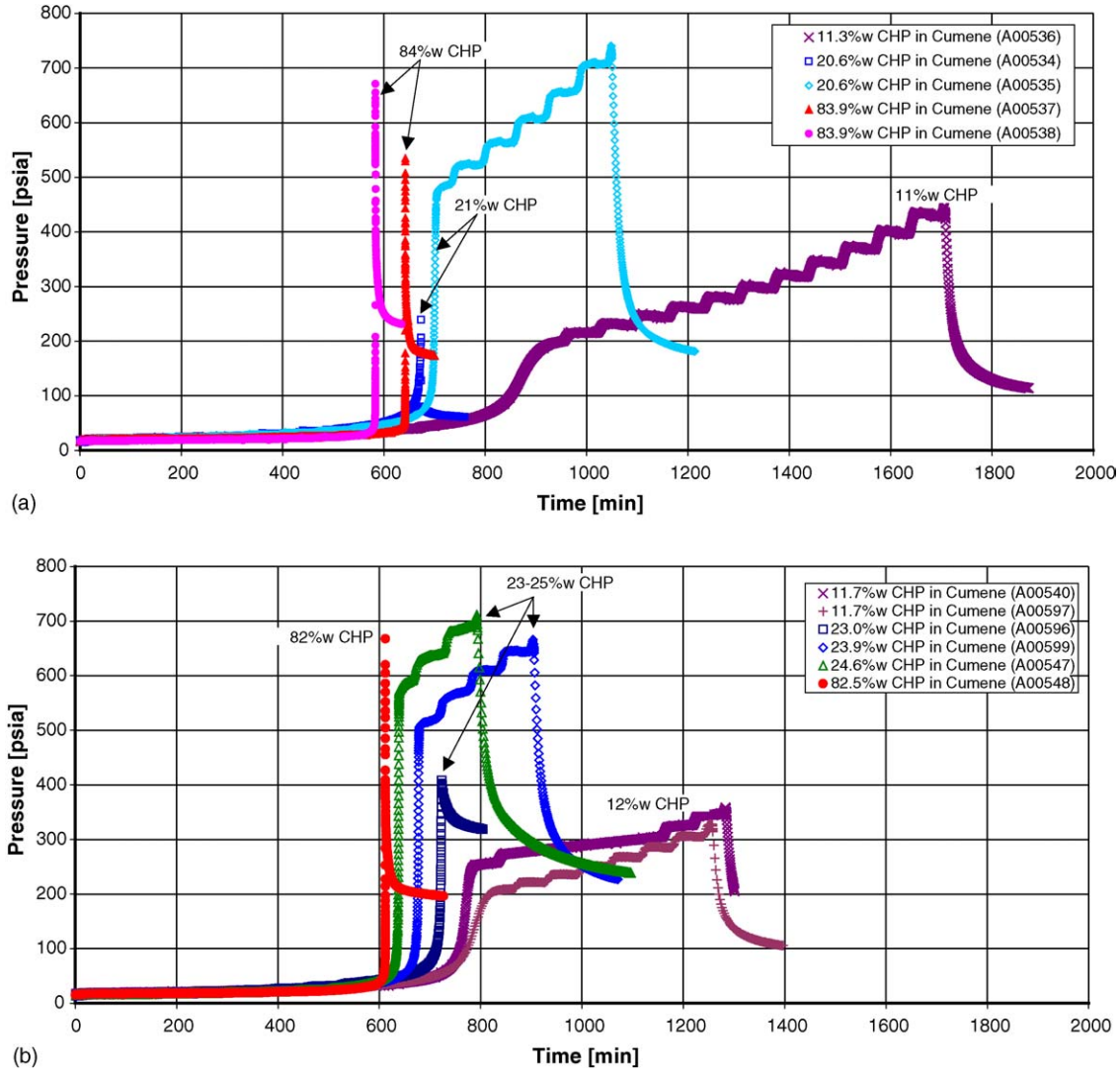

Fig. 3. Pressure–time history for CHP thermal decomposition. APTAC experiments; in nitrogen: (a) Source #1 and (b) Source #2.

Table 6
Compositional analyses of liquid product of CHP thermal decomposition tests

	Test				
	A00536	A00535	A00540	A00547	A00599
Sample source	Source #1 (wt%)	Source #1 (wt%)	Source #2 (wt%)	Source #2 (wt%)	Source #2 (wt%)
Initial CHP	11.3	20.6	11.7	24.6	23.9
CHP	<0.01	0.01	0.01	0.02	0.02
Cumene	76.4	66.1	77.2	59.6	62.6
DMBA	11.3	6.2	11.0	18.4	19.9
AP	5.4	10.4	6.0	13.2	12.4
AMS	1.6	8.7	0.98	3.8	2.5
Methanol	0.05	0.07	0.05	0.11	0.09
Phenol	0.06	0.5	0.05	0.2	0.18
Normalized on a cumene-free basis					
CHP	<0.01	0.04	0.06	0.06	0.06
DMBA	61.4	24.1	60.8	50.9	56.7
AP	29.1	40.0	33.2	36.6	35.3
AMS	8.9	33.8	5.4	10.5	7.2
Methanol	0.3	0.3	0.3	0.3	0.3
Phenol	0.3	1.8	0.3	0.6	0.5

Not able to analyze for acetone in this analysis. Acetone concentration expected to be equimolar with phenol.

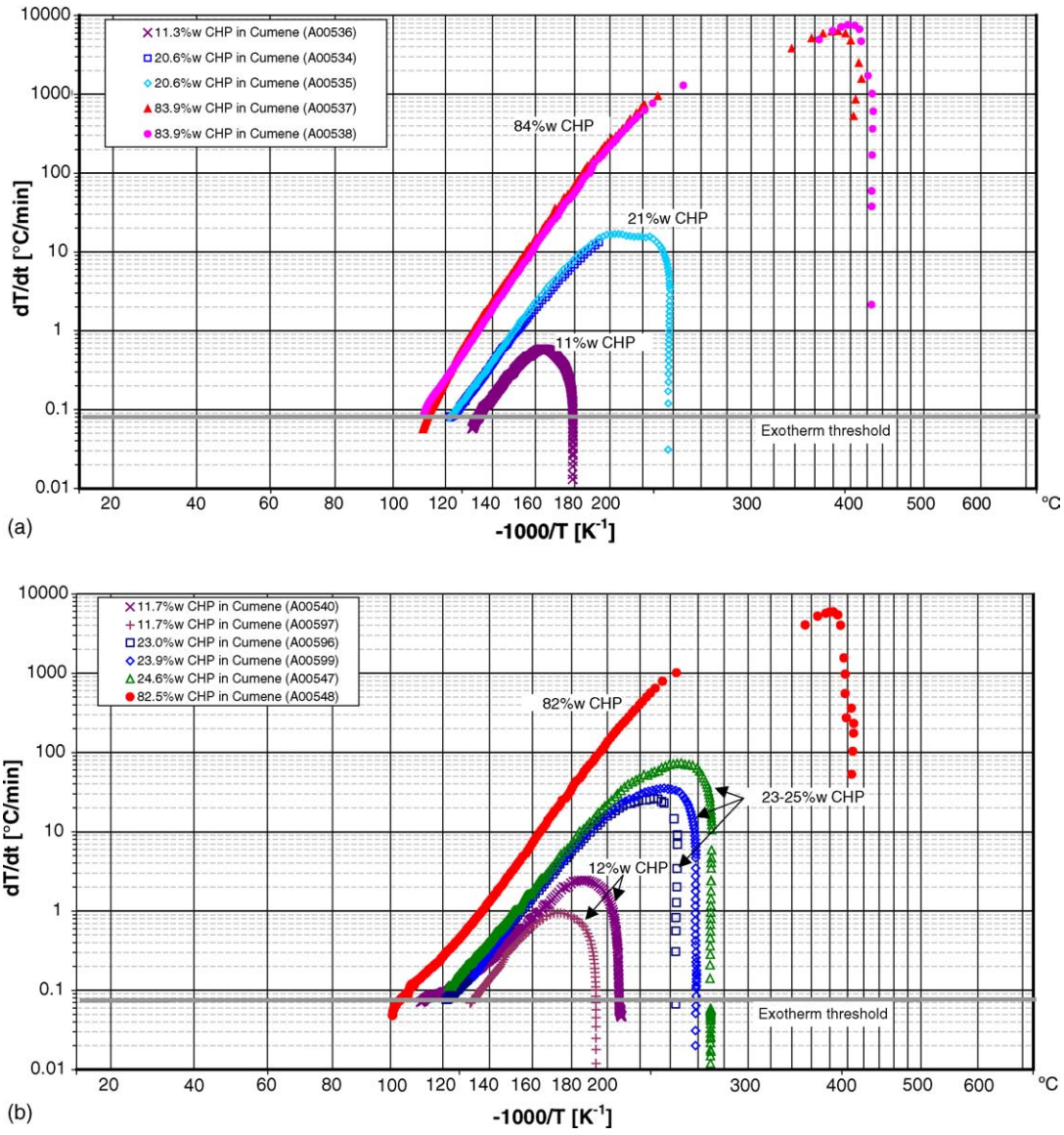

Fig. 4. Self-heat rate vs. temperature behavior for CHP thermal decomposition. APTAC experiments; in nitrogen: (a) Source #1 and (b) Source #2; heat-wait-search steps removed.

Engineers) was employed to simulate the temperature and pressure behavior of selected APTAC tests. The thermal capacitance (described earlier) of the test cell and stir bar were incorporated into the SAFIRE analysis.

For the slightly alkaline source of CHP, the following rate expressions adequately match the adiabatic calorimeter self-heat rate versus reciprocal temperature data:

CHP + cumene → 2DMBA

$$r_1 = A_1 \exp\left(-\frac{E_1}{RT}\right)[\text{CHP}][\text{Cumene}]$$

where $A_1 = 3.7 \times 10^{10}\,\text{m}^3\,\text{g mol}^{-1}\,\text{s}^{-1}$ and $E_1 = 30{,}900$ cal/(g mol).

CHP → AP + methanol

$$r_2 = A_2 \exp\left(-\frac{E_2}{RT}\right)[\text{CHP}]$$

where $A_2 = 3.8 \times 10^{12}\,\text{s}^{-1}$ and $E_2 = 32{,}300$ cal/(g mol).

For the samples derived from the slightly acidic source, similar rate expressions suffice, although the activation energies appear to be a bit lower.

CHP + cumene → 2DMBA

$$r_1 = A_1 \exp\left(-\frac{E_1}{RT}\right)[\text{CHP}][\text{Cumene}]$$

where $A_1 = 1.75 \times 10^{9}\,\text{m}^3\,\text{g mol}^{-1}\,\text{s}^{-1}$ and $E_1 = 27{,}500$ cal/(g mol).

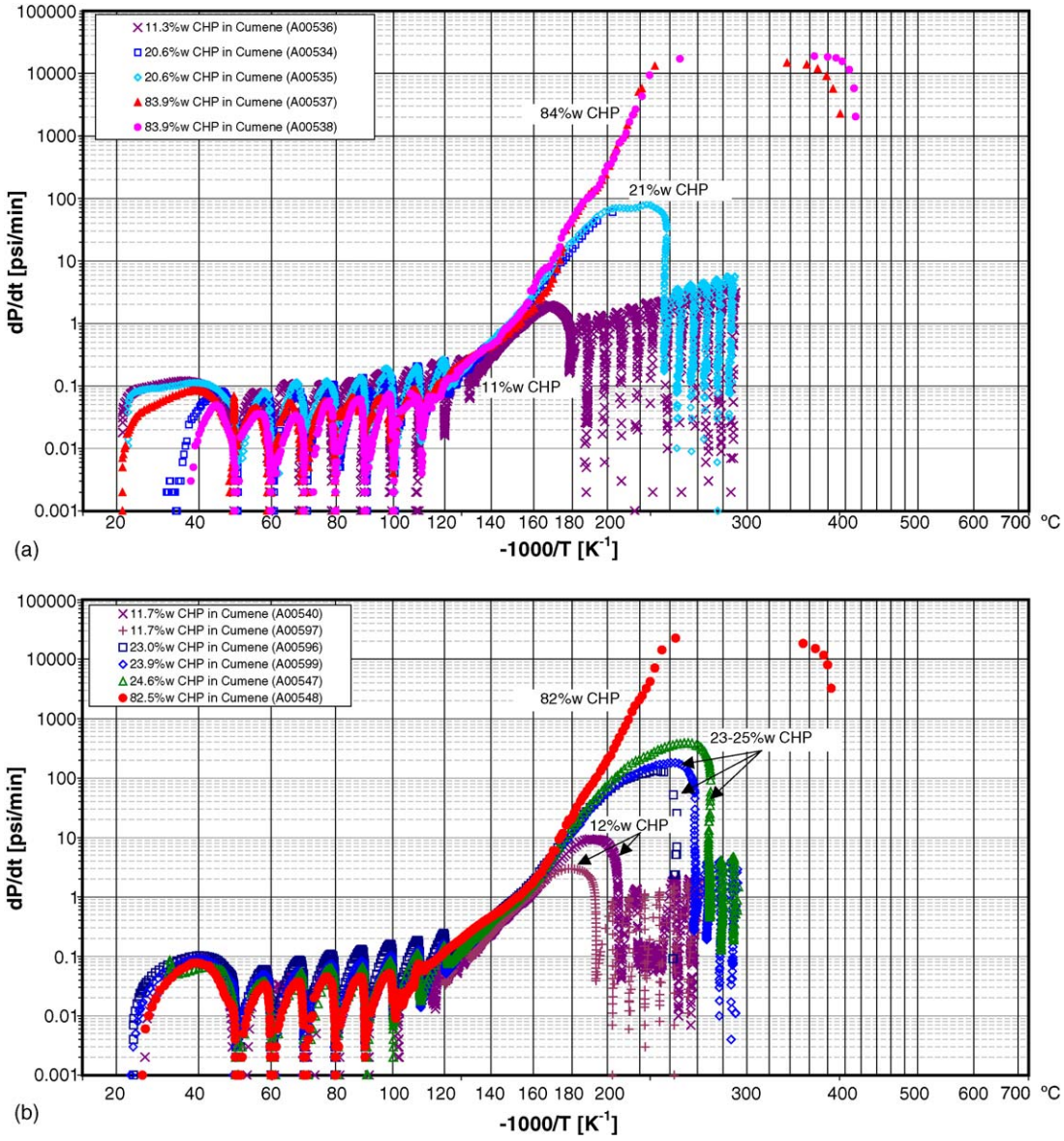

Fig. 5. Pressure rate vs. temperature behavior for CHP thermal decomposition. APTAC experiments; in nitrogen: (a) Source #1 and (b) Source #2.

$$\text{CHP} \rightarrow \text{AP} + \text{methanol}$$

$$r_2 = A_2 \exp\left(-\frac{E_2}{RT}\right)[\text{CHP}]$$

where $A_2 = 1.45 \times 10^{11}\ \text{s}^{-1}$ and $E_2 = 30{,}000$ cal/(g mol).

The rate coefficients have been adjusted to match the self-heat rate versus reciprocal temperature behavior as well as yield the observed amounts of DMBA and acetophenone. These kinetics do not account for the endothermic dehydration of DMBA to α-methyl styrene nor do they address the more recent possibility that thermal decomposition is autocatalytic [15,16]. The first-order reaction and activation energies are consistent with earlier investigations [8,9], though higher than the 1/2-order seen in other recent papers [17,18].

3.2. Acid-catalyzed cleavage of CHP

The effect of increasing concentrations of sulfuric acid on the reaction of cumene hydroperoxide is depicted in Fig. 8 in terms of temperature with time. For a nearly 25 wt% CHP concentration, the temperature at which an exotherm is detected (as evidenced by the cessation of the stair-step behavior) decreases with more concentrated acid solution. At concentrations of 8000 and 20,000 ppmw acid, the temperature is seen to rise immediately at the start of the test (that is, below room temperature). For these high concentration tests, the final temperatures also appear to be lower, reflecting an invariant heat of reaction encountered at the lower onset temperatures.

The same trend of reactivity as a function of acid content is observed for the pressure for various acid concentrations (Fig. 9). However, the extent of the pressure rise is seen to be more limited at higher acid concentrations, likely due to the reduced

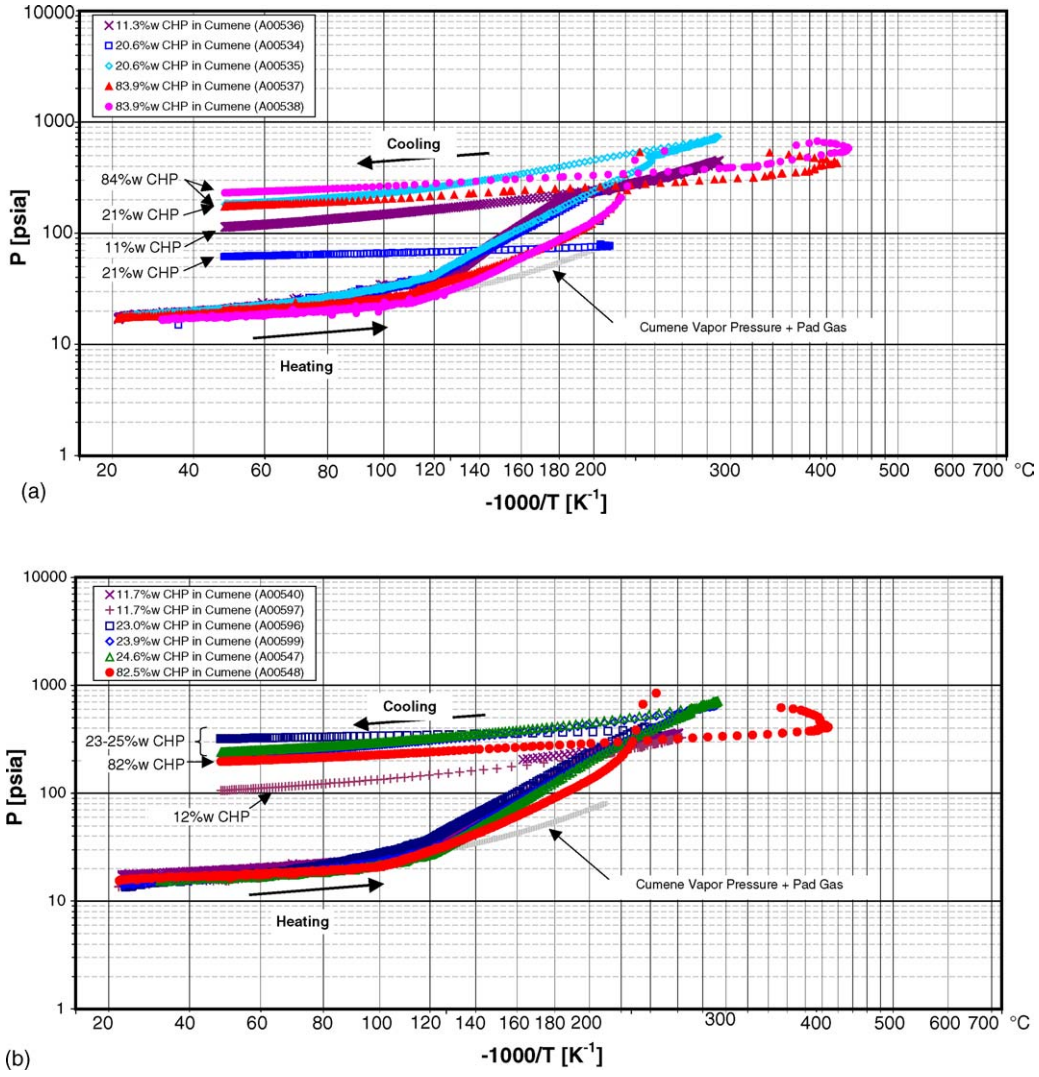

Fig. 6. Pressure vs. temperature behavior for CHP thermal decomposition. APTAC experiments; in nitrogen: (a) Source #1 and (b) Source #2.

vapor pressure at the somewhat lower final temperatures of these tests.

The influence of acid on CHP reactivity is more dramatically displayed in Fig. 10. The addition of 200–2000 ppmw sulfuric acid merely appears to shift the thermal decomposition exotherm to lower temperature. However, with 5000 ppmw or more acid, a significant exotherm emerges at temperatures below 40 °C. Though the self-heat rate of this exotherm grows rapidly with increasing temperature, it is not clear whether this behavior is actually a highly temperature-sensitive rate phenomenon or simply a reflection of the dynamics (e.g., mixing of injected acid and contacting with hydroperoxide) occurring with the reaction. It is conceivable that reaction could have taken place at lower temperatures (though the −9 °C freezing point of CHP poses a potential lower limit). For the 5000 ppmw acid tests, the low temperature exotherm is separate from the high temperature exotherm. As the acid concentration increases, the low temperature exotherm is seen to peak at a slightly higher temperature and the distinction between the low and high exotherms vanishes.

A review of the sample and nitrogen thermocouple readings reveals that, in the acid concentration tests where initial reaction rates were significant, an adiabatic environment was not always present. Bands have been added to the self-heat rate curves in Fig. 11 with arrows indicating whether the identified section should have exhibited higher or lower self-heat rate in a truly adiabatic environment. For example, since these tests were initiated at temperatures below room temperature, the initial 15 °C or so heat should have been absorbed from the ambient initially. Thus, the self-heat rates in this region of the tests should be lower than those observed. In the 5000 and 8000 ppmw acid tests, the surroundings were, at times, higher in temperature than the sample temperature in the downward segment of the first exotherm. Again, the measured self-heat rates in this portion of the first exotherm would likely be reduced in magnitude. In contrast, in several portions of the 2000–20,000 ppmw acid tests, the heaters failed to engage sufficiently, so that the gas temperature surrounding the sample cell lagged in temperature behind the sample temperature. In these parts of the exotherms, even higher self-heat rates

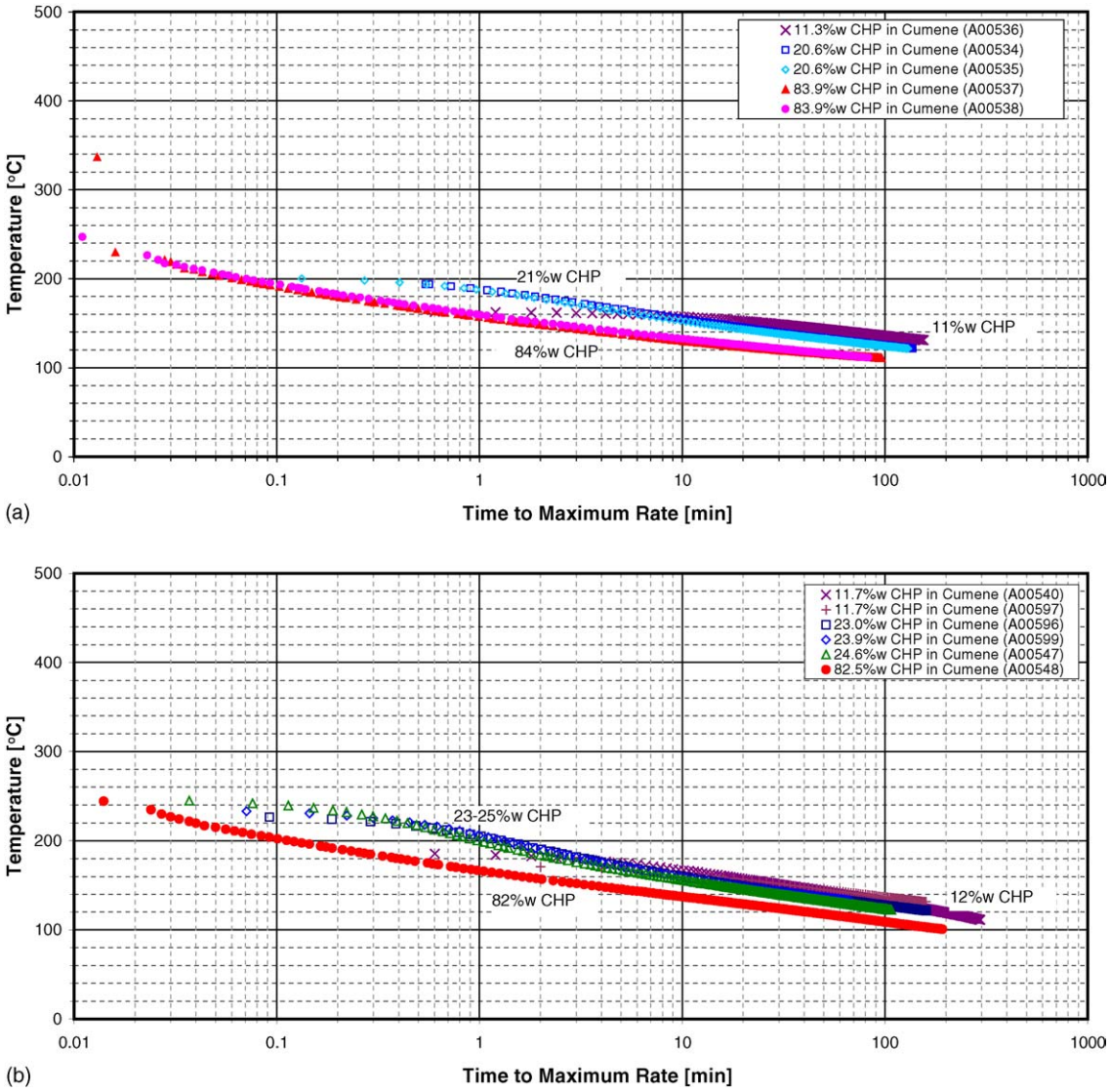

Fig. 7. Time to maximum rate for CHP thermal decomposition. APTAC experiments; in nitrogen: (a) Source #1 and (b) Source #2.

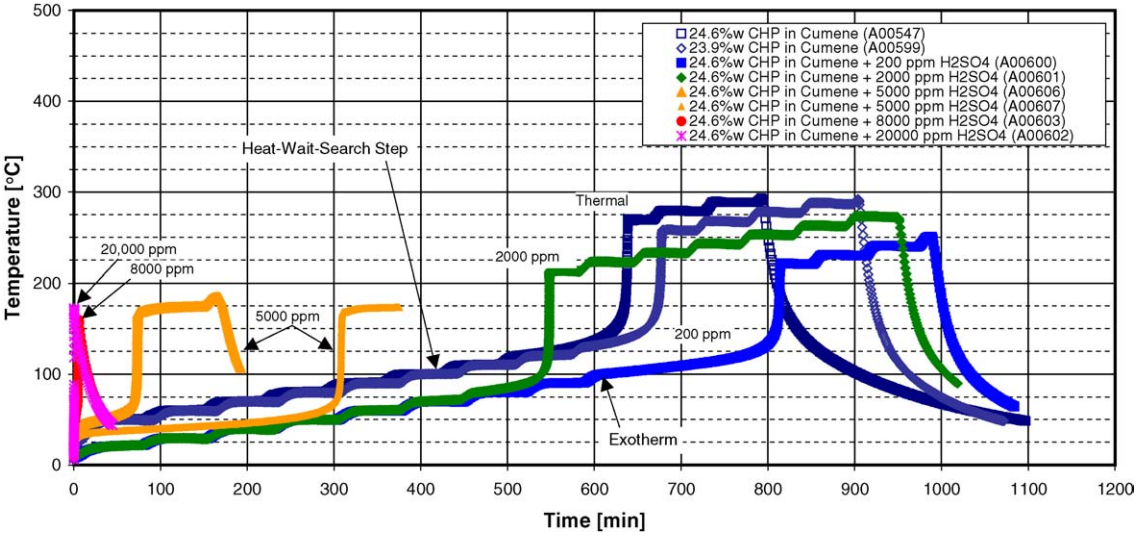

Fig. 8. Temperature–time history for CHP + acid. APTAC experiments; in nitrogen; Source #2.

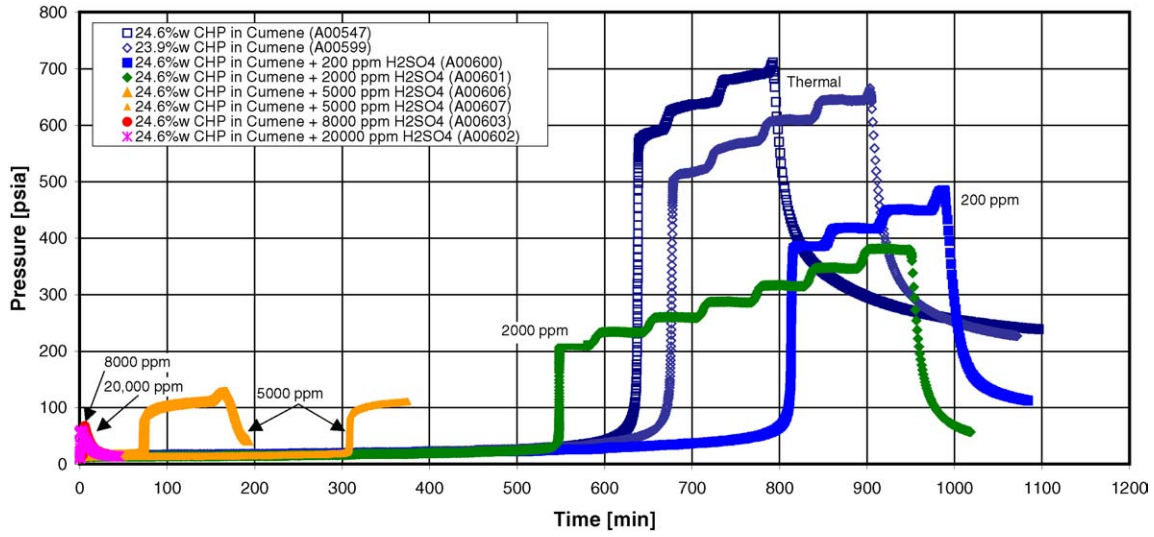

Fig. 9. Pressure–time history for CHP + acid. APTAC experiments; in nitrogen; Source #2.

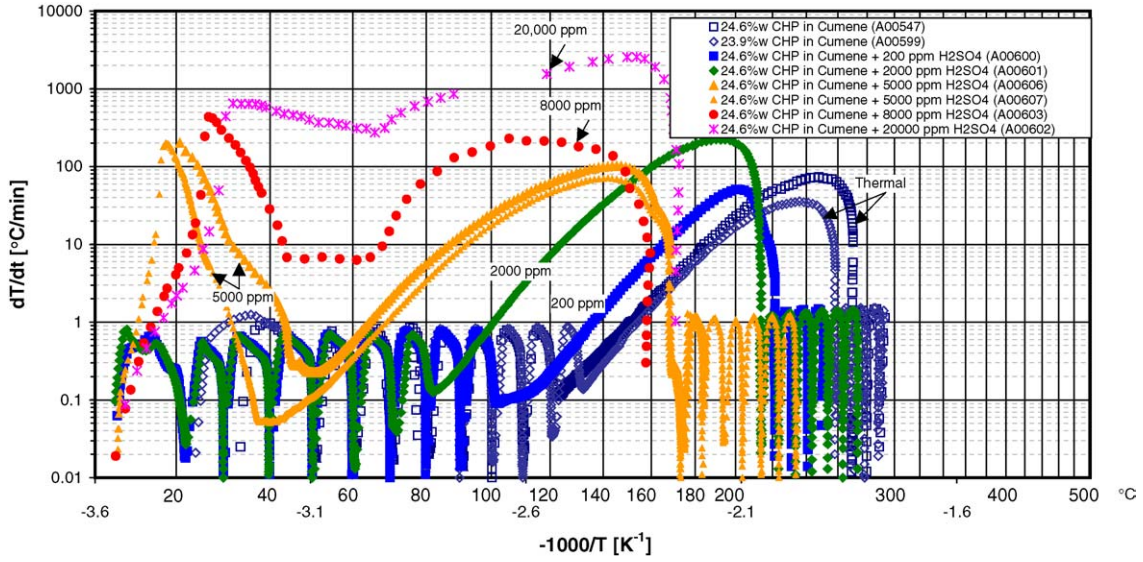

Fig. 10. Self-heat rate vs. temperature behavior for CHP + acid. APTAC experiments; in nitrogen; Source #2.

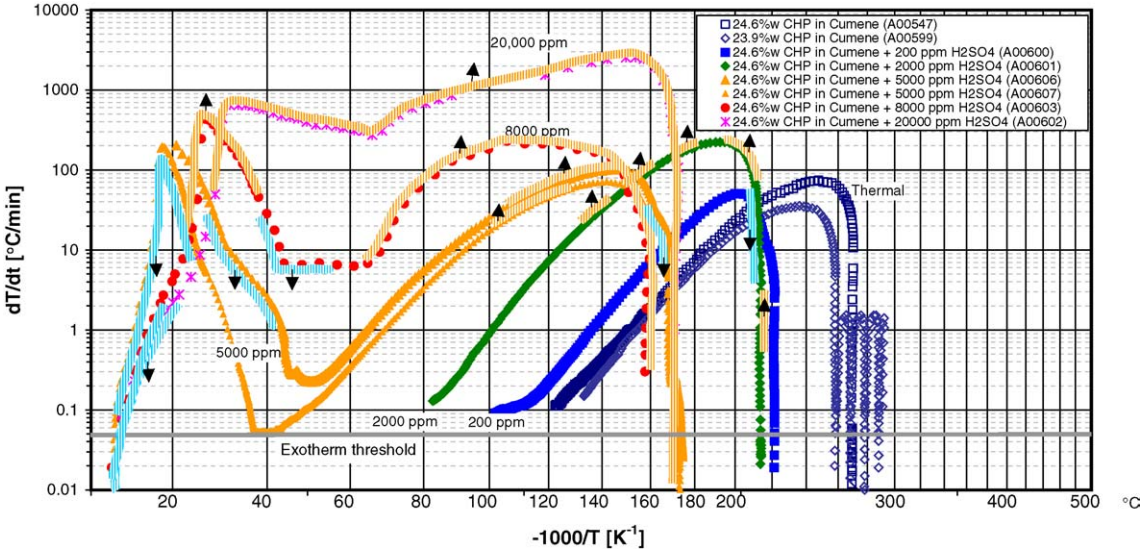

Fig. 11. Self-heat rate vs. temperature behavior for CHP + acid. APTAC experiments; in nitrogen; Source #2; heat-wait-search steps removed.

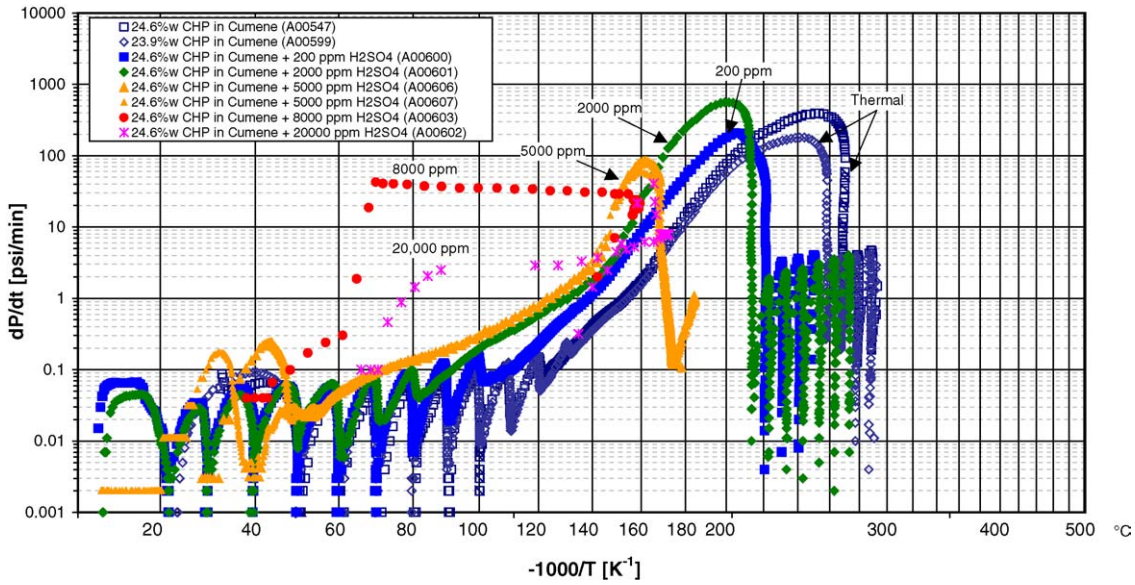

Fig. 12. Pressure rate vs. temperature behavior for CHP + acid. APTAC experiments; in nitrogen; Source #2.

could have been observed had adiabatic conditions been maintained.

Upon examination of Fig. 12, for thermal decomposition and acid-catalyzed cleavage up to 5000 ppmw sulfuric acid, the pressurization rates as a function of reciprocal temperature are strikingly similar, even displaying an upward increase in rate beyond 120–140 °C or around 1 psi/min. For the 8000 and 20,000 ppmw sulfuric acid tests, higher pressurization rates are found between 60 and 140 °C, but it is not clear why the behavior of these tests does not extrapolate from those at lower sulfuric acid concentration.

Interestingly, the residual pressure, as depicted in Fig. 13, is highest for the low acidity tests. Acetone (generated from acid-catalyzed cleavage of CHP) has a somewhat higher vapor pressure than methanol (generated from one of the thermal decomposition routes), but not enough to account for the difference observed. Since the low acidity tests have the highest final temperature, the greater residual pressure might reflect the occurrence of additional reaction(s) generating light hydrocarbons.

The time-to-maximum rate plot of Fig. 14 illustrates several curves that are generally parallel. As expected, there is a progressive reduction in the time required to reach the maximum rate as the acid concentration in the mixtures is increased. Clearly, little time is available to respond to reaction in mixtures containing CHP (ca. 25 wt%) at room temperature containing 8000 ppmw sulfuric acid or more.

Compositional analyses of the liquid product samples of selected tests are presented in Table 7. Most of the analyses were performed with a gas chromatographic method unable

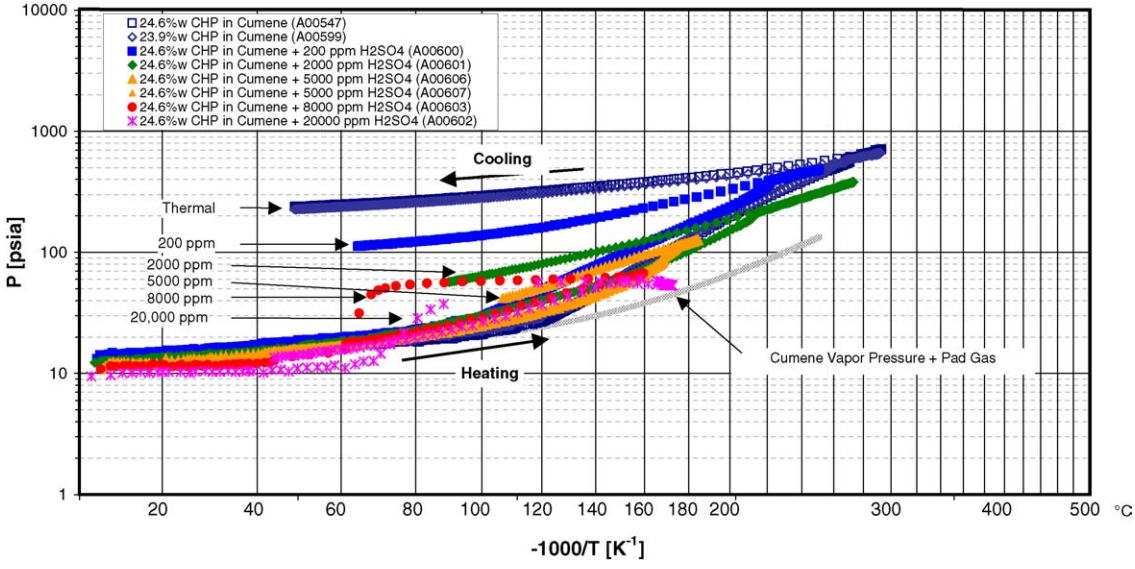

Fig. 13. Pressure vs. temperature behavior for CHP + acid. APTAC experiments; in nitrogen; Source #2.

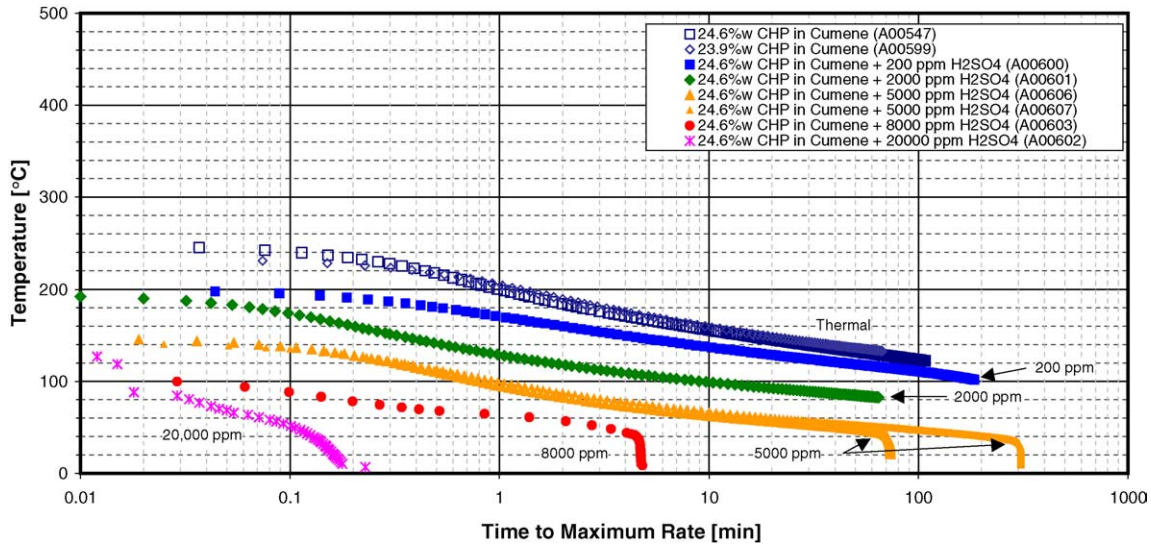

Fig. 14. Time to maximum rate for CHP + acid. APTAC experiments; in nitrogen; Source #2.

to measure acetone content. Since acetone is expected to be made in equimolar quantities with phenol, the lower half of the table provides the renormalized composition (on a *cumene-free* basis), accounting for the expected acetone (and neglecting any side reactions). It is apparent in this table that, as expected, the amount of phenol produced generally increases with the acid concentration. At the same time, the amount of acetophenone (AP) diminishes with increasing acid concentration and very little dimethyl benzyl alcohol is formed. Virtually all of the CHP is found to have reacted.

Analysis via SAFIRE simulation of the 24.6 wt% CHP (Source #2) tests with various amounts of acid has led to the following kinetics to describe the impact of acid concentration on the rate of CHP cleavage to phenol and acetone.

$$r_A = A_A\, e^{-(E_A/RT)}\, e^{m[\text{Acid}]}[\text{Acid}][\text{CHP}]^2$$

where $A_A = 8.0 \times 10^{17}$ $(m^3/kmol)^2/s$, $E_A = 36{,}000$ cal/(g mol), $R = 1.987$ cal/(g mol K), $m = 126.7$ $m^3/kmol$, T in K, [Acid] in kmol/m^3, and [CHP] in kmol/m^3.

A couple of unusual features of these kinetics are noteworthy. First, the dependence of the rate on CHP concentration is inferred to be second-order. While first-order kinetics were originally anticipated based on the concept of a single cumene hydroperoxide molecule interacting with acid, the breadth of the exotherm

Table 7
Compositional analyses of liquid product of acid-catalyzed CHP cleavage tests

	Test							
	A00600	A00601	A00607	A00603	A00602	A00604	A00614[a]	A00616[a]
Sample source	Source #2 (wt%)	Source #2 (wt%)	Source #2 (wt%)	Source #2 (wt%)	Source #2 (wt%)	Source #2 (wt%)	Source #2 (wt%)	Source #2 (wt%)
Initial CHP	24.6	24.6	24.6	24.6	24.6	10.0	10.0	4.3
Sulfuric acid	0.020	0.184	0.518	0.816	1.932	0.842	0.805	0.798
CHP	0.02	0	–	0.01	–	0	0	0
Cumene	62.9	71.2	72.7	71.4	71.6	86.8	89.7	95.7
DMBA	0	0	0.05	0.22	0	0.04	0	0
AP	7.5	2.1	0.36	0.3	0.21	0.1	0	0
AMS	7.2	3.3	0.33	1.3	0.02	0.5	0.5	0.08
Methanol	0.02	0.01	0.01	0	0	0	0	–
Phenol	3.69	11.1	10.6	13.4	12.2	5.7	6.1	2.6
Acetone	–	–	–	–	–	–	3.4	1.5
Normalized on a cumene-free basis								
CHP	0.1	0.00	0.00	0.04	0.00	0.00	0	0
DMBA	0.00	0.00	0.28	0.94	0.00	0.41	0	0
AP	36.1	9.2	2.0	1.2	1.0	0.72	0	0
AMS	34.9	14.1	1.8	5.6	0.1	4.8	5.1	1.9
Methanol	0.1	0.04	0.06	0	0	0	–	–
Phenol	17.8	47.4	59.2	57.0	61.1	58.2	58.9	62.2
Acetone	(11.0)[b]	(29.3)[b]	(36.6)[b]	(35.2)[b]	(37.7)[b]	(35.9)[b]	33.2	35.9

[a] NMR analysis.
[b] Not able to determine acetone concentration in GC analysis. Acetone concentrations estimated by assuming to be equimolar with phenol.

self-heat rate profiles clearly suggests that higher-order kinetics are more appropriate. The occurrence of second-order kinetics might derive from the possibility of CHP dimer formation at relatively low temperatures or the need for two CHP molecules to associate with acid during cleavage. Nevertheless, second-order kinetics do provide a better description of the self-heat rate versus reciprocal temperature data.

A second, atypical, and perhaps more striking attribute of these kinetics is the mixed linear–exponential dependence on acid concentration. Attempts were made to develop kinetics proportional to some power-law order in acid concentration. A greater than linear dependence on acid strength has been proposed before [19]. However, in the current study, a power-law functionality does not account for the strong sensitivity of rate with acid concentration shown by the data. The mixed linear–exponential dependence shown above works reasonably well (Fig. 15) and is consistent with functionality arising from Hammett acidity [20].

In extracting these kinetics, the previously described thermal decomposition kinetics for Source #2 were also included. Moreover, the low temperature (<40 °C) component of the high acid concentration exotherms was neglected, though the proportion of conversion of CHP in getting to 40 °C was accounted for in the modeling.

3.3. Additional investigation of acid-catalyzed cleavage of CHP

A number of tests were conducted to elucidate the exothermic behavior exhibited by CHP below 40 °C at the higher sulfuric acid concentrations. Since a mixture of 10 wt% CHP is sufficient for the exotherm to bring the final temperature to beyond 40 °C (up to 80 °C), this concentration served as the basis for many of the investigatory tests. In addition, an experiment at about 4 wt% CHP was conducted since this amount of hydroperoxide brings the temperature up to about 40 °C before terminating.

The low temperature exotherm is found to occur for concentrations of 5000 ppmw sulfuric acid and higher. A number of potential factors are considered in assessing this behavior: instrument reliability; exotherm shape if the experiment could have begun at a lower temperature; possible mass transfer limitations during sulfuric acid injection; solubility effects; complex reaction pathways with impact on thermodynamics and kinetics.

The rapid rise in self-heat rate at the start of the test suggests the possibility of a mass transfer limitation (i.e., contact of sulfuric acid with the cell contents after its injection) or an autocatalytic effect. It might simply reflect that the reaction was already moving too rapidly at the starting temperature of the test. The additional "humps" in the self-heat rate profile following the initial spike in rate might indicate the presence of other reaction steps taking place. As more acid is added, the magnitude of these intermediate peaks grows in intensity. In any event, the shape of the self-heat rate profile between the start of the test and 40 °C, that is, rising quickly and falling off more gradually, is quite distinct from the "classical" shape exhibited for power-law kinetics in an adiabatic calorimeter [21].

The low temperature exotherm appears when sulfuric acid is added to concentrations of 24.6, 10, or 4.3 wt% CHP (Fig. 16). The phenomenon appears to be associated with high acid concentrations in combination with some amount of hydroperoxide. As found in Table 7, even with the 4.3 wt% CHP sample, the primary products were still phenol and acetone (i.e., even with low initial CHP concentration, no other significant reaction products were found that might suggest a different reaction pathway at low temperatures).

It is clear from Fig. 10 that the low temperature reaction phenomenon occurs only at the elevated sulfuric acid concentrations (there might even be a hint of the exotherm at 2000 ppmw). In a supplemental test, 20,000 ppmw sulfuric acid was added to neat cumene (that is, with no CHP). The low temperature behavior up to 40 °C was not observed at all. This suggests that the low temperature exotherm is

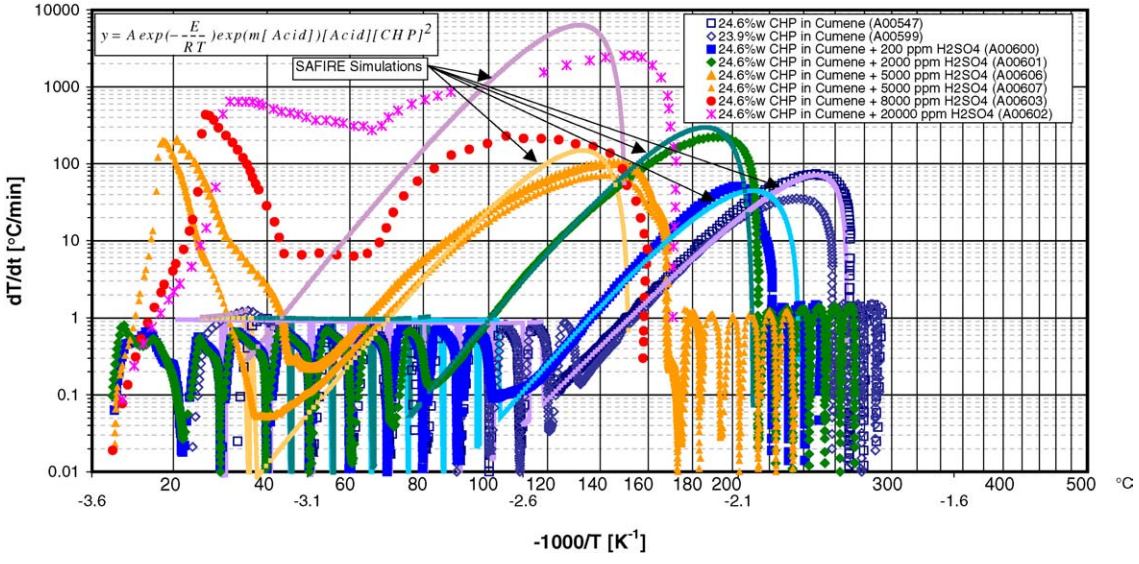

Fig. 15. Comparison of acid-catalyzed kinetic model with self-heat rate behavior for CHP + acid; SAFIRE.

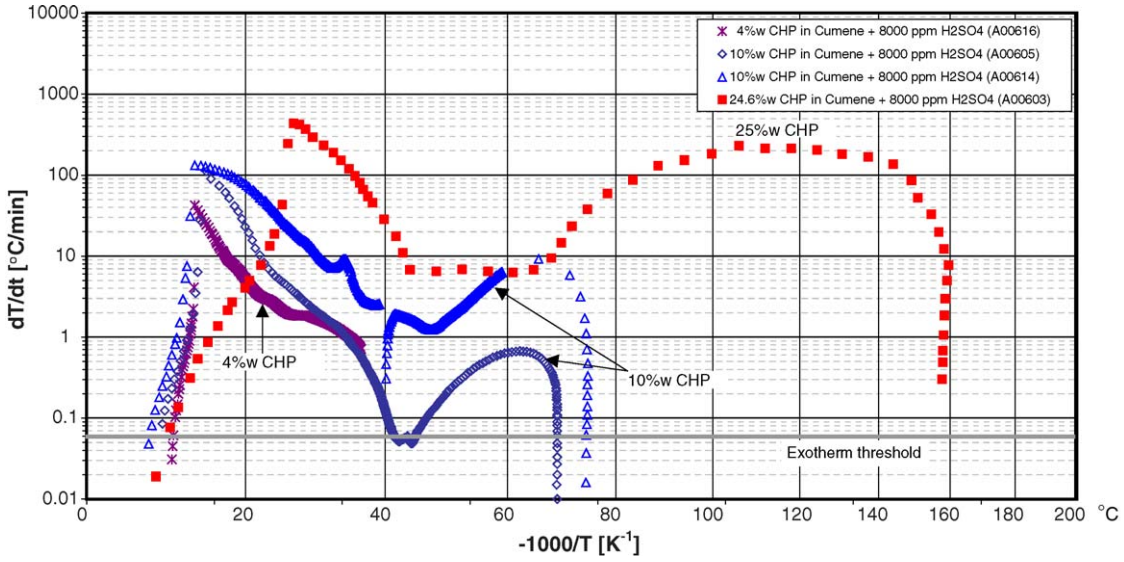

Fig. 16. Self-heat rate dependence on concentration for CHP + acid. APTAC experiments; in nitrogen; Source #2; heat-wait-search steps removed.

not merely an instrument artifact associated with high acid concentrations.

In another test, ethylbenzene sulfonic acid was injected instead of sulfuric acid into a mixture containing 10 wt% CHP. Ethylbenzene sulfonic acid is considered representative of a possible species formed when sulfuric acid is introduced to aromatics such as cumene. The amount of sulfonic acid injected was chosen to be equivalent, on a molar sulfur basis, to 8000 ppmw sulfuric acid. In this test, a rapid rise in self-heat rate below 20 °C was also observed. This exotherm experienced a reduction in rate prior to onset of the more classical exotherm above 30 °C (Fig. 17). These results, as do the findings from the sulfuric acid plus cumene test, indicate that the lowest temperature behavior does not arise from association of sulfuric acid itself with aromatics. It is still conceivable that association of the hydroperoxide with the acid might be responsible for the observed behavior.

In another test, reaction of 24.6 wt% CHP with 5000 ppmw sulfuric acid was initiated and terminated at 30 °C; that is, far below the expected final temperature of around 170 °C. The sample was then cooled back to below 10 °C and allowed to re-heat. In the first test, the low temperature exotherm took place as usual. Upon restarting at low temperature, the low temperature behavior was completely absent, leading to a conclusion that the low temperature exotherm is not thermodynamically reversible nor a reaction that would necessarily continue to occur if the temperature were kept low. It seems that the low temperature reaction ran its course and no further amount would take place.

Several more tests were performed to characterize the impact of cleavage product, namely phenol and acetone, on reaction

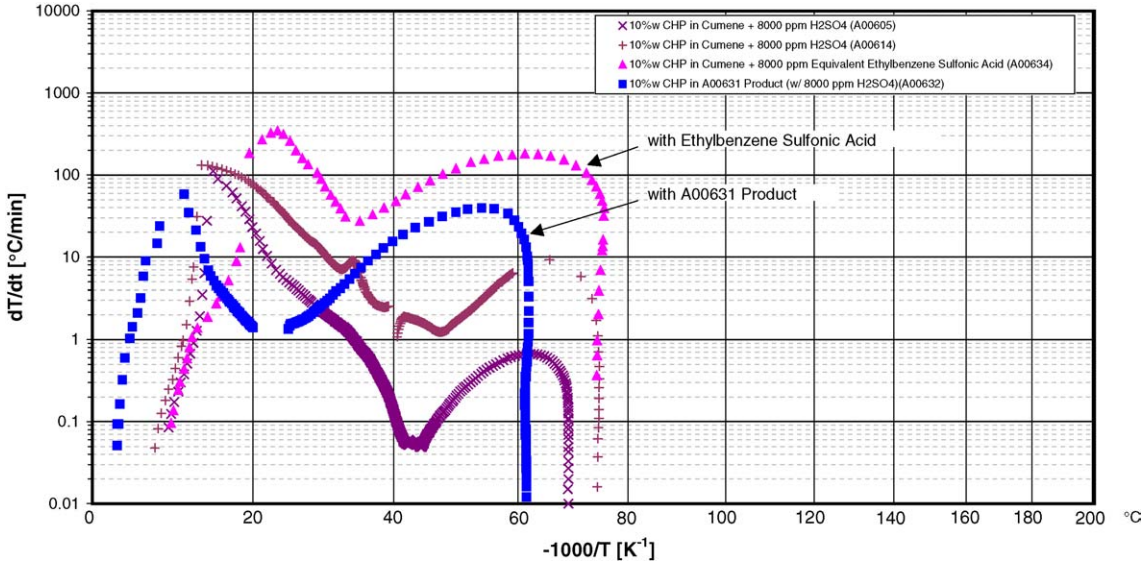

Fig. 17. Self-heat rate variation with conditions for CHP + acid. APTAC experiments; in nitrogen; Source #2; heat-wait-search steps removed.

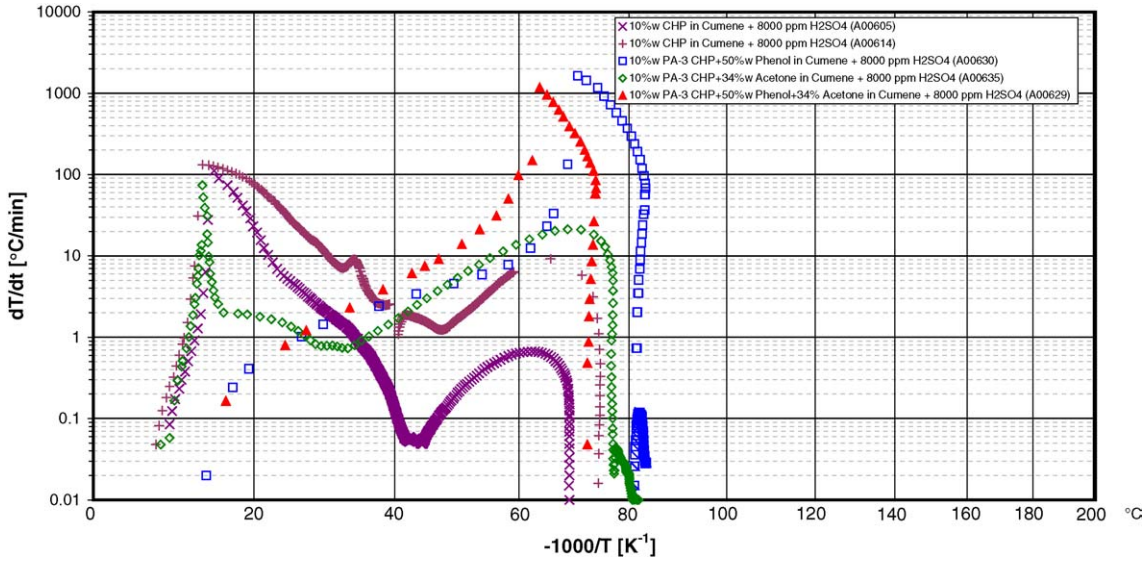

Fig. 18. Self-heat rate dependence on phenol and acetone content for CHP + acid. APTAC experiments; in nitrogen; Source #2; heat-wait-search steps removed.

behavior. In one test, in which 8000 ppmw sulfuric acid was injected into 10 wt% CHP, the low temperature reaction was allowed to finish. Following completion of the exotherm, the test cell was allowed to cool back to ambient temperature. Afterwards, the test cell was cooled in a water/ice bath and 7.55 g of 82.46 wt% CHP (Source #2) was injected to bring the sample CHP concentration back up to about 10 wt% (but now with phenol and acetone product present in concentrations under 10 wt% each). Except for the lower test start temperature (merely a function of how much time transpires between removal of the water/ice bath and start of run) leading to a lower end temperature, the test results qualitatively parallel those of other 10 wt%/8000 ppmw sulfuric acid experiments. It also appears that more of the exotherm is shifted toward the higher temperature, more classical power-law shaped exotherm in this run (Fig. 17).

Exploring the effect of phenol and acetone on reactivity further, a test was performed in which much of the cumene was replaced with phenol, yielding a mixture containing 50 wt% phenol. In this case, the rate of the low temperature exotherm, particularly below 30 °C, was dramatically reduced (Fig. 18). This was also the case when the mixture was formulated to contain 50 wt% phenol and 34 wt% acetone. The 40–80 °C exotherm also exhibits a sharp additional peak reflecting a much increased rate. In contrast, though, when the mixture has 34 wt% acetone and *no* phenol, the low temperature peak narrows, yet has the same order of magnitude rate as when no acetone is present. A smaller peak follows leading into the classical 40–80 °C exotherm.

In short, it appears that the low temperature exotherm, whose shape reflects more phenomena occurring than just power-law kinetics, occurs only with the combination of elevated concentrations of sulfuric acid with CHP and is inhibited by the presence of phenol. It is speculated that the behavior arises, in part, from association of the acid with the hydroperoxide, while production of phenol and acetone still occur.

3.4. Thermal inertia effects

In this study's experiments, the thermal inertia or phi factor, ϕ, ranges between 1.25 and 1.31 (see Tables 2–5). This means that the sample container has a thermal capacitance of 25–31% of that of the sample, or expressed differently, about 20–24% of the total of the cell plus sample. The *actual* temperature rise experienced in a large-scale adiabatic environment, in which the *relative* wall thermal capacitance might be very small, would be higher by the thermal inertia factor or an additional 25–31%. Thus, the extent of each exotherm would be greater than that seen from the test data and may hasten the transition between exotherms. Furthermore, a greater pressure build-up can be expected to accompany the increased temperature rise. In addition to the impact of thermal inertia on temperature rise, the self-heat rates associated with the exotherms would be greater at the commercial scale than those observed in the experiments by a factor larger than the thermal inertia factor. This means that the timeframe for a temperature/pressure excursion beginning at some initial temperature would be correspondingly shorter.

To adjust the current study's results properly for equipment with a lower thermal inertia, a dynamic simulation that takes into account the observed reaction kinetics coupled with material and equipment properties, such as that performed to extract the kinetics reported earlier, would be required.

4. Summary

The reactivity of cumene hydroperoxide undergoing thermal decomposition and acid-catalyzed cleavage has been examined. Samples of CHP were obtained from slightly acidic and slightly basic sources. Subtle differences were revealed in the behavior of these samples. Overall, though, first-order decomposition to acetophenone and overall second-order decomposition to dimethyl benzyl alcohol (first order in CHP, first order in cumene) are consistent with the experimental results.

When a CHP mixture contains small amounts of sulfuric acid, the exotherm is observed to shift to lower temperature. With increasing concentration of acid, the exotherm profile continues to move toward lower temperatures. This shift translates into an increase in reaction rate that is much stronger than power-law dependence on acid concentration. A combined linear multiplied by exponential function of acid concentration provides an adequate characterization of the acid-catalyzed reactivity.

For acid concentrations at or above 5000 ppmw, an exotherm emerges at a temperature as low as 5 °C. This exotherm only appears at the elevated acid concentrations and when CHP is present. It does not bear a shape characteristic of power-law kinetics for reactions in adiabatic conditions and its shape might be influenced by a relatively high starting test temperature, mass transfer effects, or complex kinetics. An intermediate exotherm also follows and grows in intensity with acid concentration. The presence of phenol tends to diminish the low temperature reaction.

References

[1] R.T. Morrison, R.N. Boyd, Organic Chemistry, fifth ed., Allyn and Bacon, 1987.
[2] M. Hronec, A. Stasko, L. Malik, A.S. Herrera, Oxid. Commun. 3 (2) (1983) 125–134.
[3] G.J. Suppes, M.A. McHugh, Ind. Eng. Chem. Res. 28 (1989) 1146–1152.
[4] Y.-W. Wang, C.-M. Shu, Y.-S. Duh, C.-S. Kao, Ind. Eng. Chem. Res. 40 (2001) 1125–1132.
[5] K. Ohkubo, T. Yamabe, K. Fukui, Bull. Chem. Soc. Jpn. 43 (1970) 1–8.
[6] T.C. Ho, Y.-S. Duh, J.R. Chen, Case studies of incidents in runaway reactions and emergency relief, in: AIChE Loss Prevention Symposium, March 1998.
[7] Marsh, The 100 Largest Losses 1972–2001: Large Property Damage Losses in the Hydrocarbon-Chemical Industries, 20th ed., February 2003.
[8] J.R. Thomas, J. Am. Chem. Soc. 77 (1955) 246–248.
[9] R. Rado, I. Chodák, Collection Czechoslov. Chem. Commun. 38 (1973) 2614–2620.
[10] A.W. de Ruyter van Steveninck, E.C. Kooyman, Recueil des Travaux Chimiques des Pays-Bas et de la Belgique 79 (1960) 413–429.
[11] M. Weber, DGMK-Conference, Erlangen, 1999, pp. 239–245.
[12] L. Pellegrini, S. Bonomi, G. Biardi, Identification of risk scenarios in the phenol–acetone process. Part II: The cumene hydroperoxide cleavage section, in: Presentation to the AIChE 37th Annual Loss Prevention Symposium, New Orlean, LA, 2003.
[13] M.E. Levin, A.D. Hill, Reactivity of Unsaturated Hydrocarbons via Adiabatic Calorimetry, in: Proceedings of the 2000 Mary Kay O'Connor Process Safety Center Annual Symposium, 2000.
[14] M.E. Levin, A.D. Hill, The reactivity of butadiene with acetylenic hydrocarbons via adiabatic calorimetry, in: Proceedings of the 2001 Mary Kay O'Connor Process Safety Symposium, October 30–31, 2001.
[15] A. Miyake, M. Sumino, Y. Oka, T. Ogawa, Y. Iizuka, Thermochim. Acta 352–353 (2000) 181–188.
[16] H.-Y. Hou, C.-M. Shu, Y.-S. Duh, AIChE J. 47 (8) (2001) 1893–1896.
[17] Y.-S. Duh, C.-S. Kao, C. Lee, S.W. Yu, Trans. IChemE 75 (1997) 73–80.
[18] Y.-S. Duh, C.-S. Kao, H.-H. Hwang, W.-L. Lee, Trans. IChemE 76 (Part B) (1998) 271–276.
[19] C. Iditoiu, E. Segal, B.C. Gates, J. Catal. 54 (1978) 442–445.
[20] T.H. Lowry, K.S. Richardson, Mechanism and Theory in Organic Chemistry, third ed., Harper & Row, 1987.
[21] D.I. Townsend, J.C. Tou, Thermochim. Acta 37 (1980) 1–30.